A Probability Description of the Yule-Nielsen Effect

J. S. Arney*
Center for Imaging Science, Rochester Institute of Technology
Rochester, New York 14623

Abstract

The Yule-Nielsen effect, also called optical dot gain, has often been modeled based on convolutions between halftone dot patterns and a point spread function, PSF, characteristic of the paper. The form of the PSF is generally assumed or measured empirically. An alternative approach to modeling the Yule-Nielsen effect employs a probability function P_p, which describes the fraction of reflected light emerging between halftone dots and under dots. The probability model is shown to fit experimental data on the Yule-Nielsen effect quite well. Moreover, the model can be implemented with simple algebraic expressions rather than the convolution or Fourier calculations required for PSF models. In addition, the quantitative relationship between P_p and PSF is demonstrated.

Introduction

Most printing processes print ink onto paper at only one level, and gray scale is achieved by printing patterns of dots and varying the fraction F of the paper covered with the dots. Murray and Davies modeled gray scale in printed halftone dots with the following expression,[1]

$$R(F) = FR_i + (1 - F)R_p, \tag{1}$$

where R, R_i, and R_p are, respectively, the mean level reflectance of the image, the reflectance of the printed ink, and the reflectance of the not printed paper. However, variation from this simple linear model is typically observed and is often called the Yule-Nielsen effect.[2] Figure 1 illustrates the Yule-Nielsen effect for a 65-lpi, clustered-dot-halftone gray scale printed with a wax thermal printer with 300-dpi addressability.

Yule and Nielsen suggested the following function to model the effect,

$$R(F) = [FR_i^{1/n} + (1 - F)R_p^{1/n}]^n, \tag{2}$$

where n is an empirical constant adjusted to fit the experimental data,[2] as illustrated in Fig. 1. Subsequent work by Yule and others has examined the fundamental relationship between the n factor and independently measurable parameters of the ink and the paper.[3–5] The focus of the current report is to contribute to this understanding by exploring a probability-based model of the Yule-Nielsen effect similar to that suggested by Huntsman.[6]

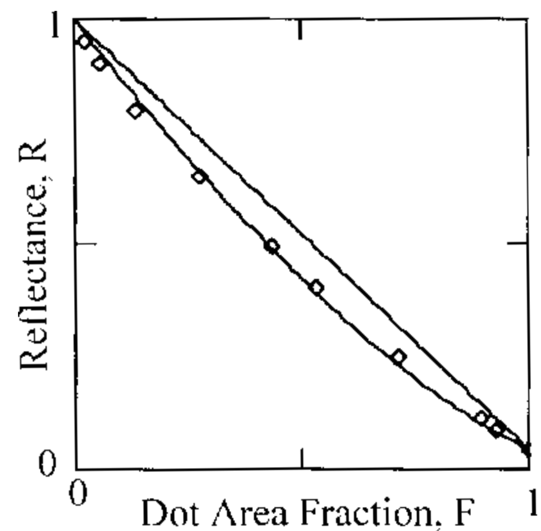

Figure 1. Reflectance of 65-lpi clustered halftone pattern versus dot area fraction. Lines for the Murray-Davies Eq. 1 and for the Yule-Nielson Eq. 2 with n = 1.5 are shown.

The assumptions employed in this report include (1) clustered dot halftones, (2) no penetration of the dot into the paper substrate, (3) negligible scattering within the dot, and (4) negligible effects from multiple specular reflections between the ink dots and the paper. The intent is to lay the foundations for later investigations of the impact of varying from these assumptions. Experimental data in this report were obtained using a calibrated CCD camera, microscope optics, frame grabber, and analysis software as described previously.[7]

Light Scattering

Yule and Nielsen pointed out that the fundamental reason for the nonlinear relationship between R and F is the lateral scattering of light within the paper.[2–4] Light that enters the paper between halftone dots scatters laterally, and this lateral motion of the light in the paper increases the probability the light will encounter an ink dot and be absorbed. Published reports relating the Yule-Nielsen effect to paper and ink parameters have employed one of two models: The first and most common modeling approach describes the lateral motion of the light in

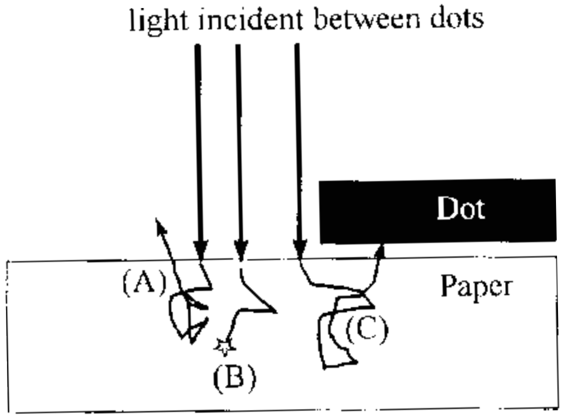

Figure 2. Photons entering the paper between the dots may be absorbed (b), return to the surface between the dots (a), or under a dot (c).

paper with a point spread function PSF or the Fourier equivalent, the modulation transfer function MTF.[4, 8–12] Oittinen[13] and Engeldrum[14] have derived the MTF from Kubelka-Munk theory, but a useful empirical model of the paper MTF[15] and its corresponding PSF are as follows:

$$\mathrm{MTF}(\omega) = \frac{1}{1+(k_p\omega)^2}, \tag{3}$$

$$\mathrm{PSF}(x) = \frac{1}{k_p} K_0\left(\frac{2\pi x}{k_p}\right), \tag{4}$$

where x is the distance in mm from the point where light enters the paper, w is spatial frequency in mm^{-1}, k_p is a constant proportional to the mean lateral distance light travels in the paper, and K_0 is a Bessel function of the third kind.[16] The interaction between the light and the halftone dots can be modeled using a convolution integral between the dot pattern $f(x)$ and the point spread function PSF(x). Several excellent examples of this approach to halftone modeling have been published, including studies of the impact of the Yule-Nielsen effect on the color gamut in printed halftones.[4, 8–12]

A Probability Model

An alternative approach for modeling the Yule-Nielsen effect is based on probability functions for photon behavior in paper, as suggested by Huntsman.[6] For example, as illustrated in Fig. 2, a photon entering the paper between halftone dots will have a finite probability R_g of returning to the paper surface as a reflected photon. The term R_g is also the optical reflectance factor of the paper. The photon can emerge between dots, (A) in Fig. 2, or under a dot, (C) in Fig. 2. As pointed out by Huntsman, we can identify the probability P_p of these photons returning to the surface under a halftone dot and a probability $1 - P_p$ of their returning to the surface between the dots. We may also consider the photons that strike the halftone dots of transmittance T_i. These photons have a probability T_i of entering the paper, and then a probability R_g of returning to the surface of the paper. Of those returning to the surface, there is a probability P_i of returning to the paper surface under a halftone dot and a probability $1 - P_i$ of returning to the surface between the dots. These probabilities are summarized in Table I. Based on probability accounting of this kind, Huntsman was able to derive the Murray-Davies Eq. 1. Moreover, Hunstman's derivation demonstrated R_i and R_p are not constants as assumed in both Eqs. 1 and 2, but are functions of the dot area fraction F.

TABLE I. Probability of Photons Returning to the Surface

Probability of Emerging	Route of Entry Into Paper: Under Dot	Route of Entry Into Paper: Between Dot
Under Dot	(a) P_i	(b) P_p
Between Dot	(c) $1 - P_i$	(d) $1 - P_p$

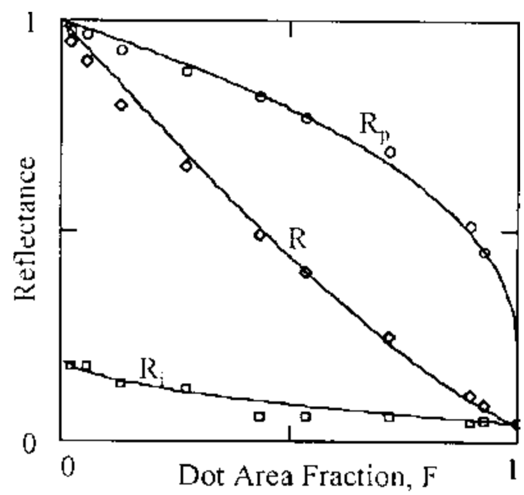

Figure 3. Empirical model of Eqs. 5, 6 and 1 fit to data on paper reflectance R_p ink reflectance R_i and man reflectance, R, versus dot area fraction for a 65-lpi clustered halftone pattern printed with a 300-dpi wax thermal transfer printer on a calendered, noncoated paper.

Experimental observations of the variation of both R_i and R_p with F have been reported,[7,17] and the data in Fig. 3 are an example. The data were obtained for a 65-lpi clustered-dot halftone printed with a wax thermal printer at 300-dpi addressability, and the data were measured with a CCD camera, microscope, frame grabber, and analysis software as described previously.[7] By analogy with Yule-Nielsen, the data in Fig. 3 were fit to the following empirical functions for R_i and R_p by varying an arbitrary power factor w. The value T_i is a constant equal to the transmittance of the ink dot.

$$R_p = R\,[1 - (1 - T_i)\,(1 - (1 - F)^w)], \tag{5}$$

$$R_i = R_g T_i [1 - T_i) F^w]. \quad (6)$$

The resulting R_i and R_p values were used with Eq. 1 to model the overall reflectance R versus F.

Earlier work demonstrated a relationship between the empirical model of Eqs. 5 and 6 and the MTF/PSF model represented by Eqs. 3 and 4.[8,15] In particular, the power factor w and the mean free path k_p are related as follows:

$$w = 1 - e^{-A k_p f}, \quad (7)$$

where f is the dot frequency of the halftone pattern. The constant A was determined empirically by fitting Eq. 7 to experimentally measured values of w versus $k_p \cdot f$. As suggested in previous a work by Huntsman,[6] the value of the constant A depends on the shape and distribution of the halftone dots. An experimental study of this effect is currently underway. In the current report, the physical significance of Eqs. 5 and 6 is examined by further development of the probability model suggested by Huntsman.

Paraphrasing the Huntsman Model

The notation used in the following derivation differs from Huntsman,[6] but the thrust of the arguments is the same. We begin with an incident irradiance I_o onto the halftone sample. The relative flux of photons striking the dots and the paper between the dots is $F \cdot I_o$ and $(1 - F) \cdot I_o$, respectively. The dot decreases the flux of photons entering the paper to $T_i \; F \; I_o$. With absorption by the paper R_g and scattering governed by the probabilities P_i and P_p, the number of photons emerging as reflectance at the surface of the paper can similarly be expressed as shown in Table II. The total flux of photons emerging from the paper between the dots, I_p, is the sum of the terms in cells (c) and (d) of Table II.

$$I_p = R_g I_0 [F_i T_i (1 - P_i) + (1 - F)(1 - P_p)] \quad (8)$$

In order to obtain the observed reflectance of the paper between the dots, we divide Eq. 8 by the flux incident on the paper between the dots, $I_o (1 - F)$. The result shows R_p as a function of the dot area fraction, F.

$$R_p = R_g \left[T_i (1 - P_i) \left(\frac{F}{1 - F} \right) + (1 - P_p) \right] \quad (9)$$

Similarly, the reflectance of the dot is as follows.

$$R_i = R_g T_i \left[P_i T_i + P_p \left(\frac{1 - F}{F} \right) \right] \quad (10)$$

Thus, if we knew the probability functions, P_i and P_p, then R_i and R_p could be calculated, and then with Eq. 1 the overall halftone reflectance could be calculated.

Intuitively, the two probabilities P_i and P_p must be related. We can gain some insight into this relationship by examining a special case of $T_i = R_g = 1$. In this case we know $R_i = R_p$ so we can equate Eqs. 9 and 10. By rearranging the result we obtain a relationship between P_i, P_p, and F.

TABLE II. Summary of Reflected Photon Flux Between and Under Halftone Dots.

Flux Emerging	Route of Entry Into Paper: Under Dot	Route of Entry Into Paper: Between Dot
Under Dot	(a) $P_i I_0 T_i F R_g$	(b) $P_i I_0 R_g (1–F)$
Between Dot	(c) $(1 – P_i) I_0 T_i F R_g$	(d) $(1 – P_p) I_0 R_g (1–F)$

$$P_i = 1 - P_p \left(\frac{1 - F}{F} \right). \quad (11)$$

This relationship is true for $T_i = R_g = 1$. The generality of Eq. 11 can be extended by recognizing that P_i and P_p are independent of the total number of photons scattering about in the paper, so that the probabilities are independent of T_i. We also will assume they are independent of R_g, although it has been shown the mean free path in paper is a function of absorption as well as scattering.[13, 14] Thus, Eq. 11 is assumed true for all values of T_i and R_g.

By substitution of Eq. 11 into Eqs. 9 and 10, we obtain the following two expressions for R_i and R_p.

$$R_p = R_g [1 - P_p (1 - T_i)], \quad (12)$$

$$R_i = R_g T_i \, [1 - P_i (1 - T_i)]. \quad (13)$$

Equations 1 and 11 through 13 provide a model for tone reproduction. Three things are needed: constants for R_g and T_i and knowledge of the probability function P_p. If P_p is known, then the function P_i is determined with Eq. 11. Then P_p and P_i are used with Eqs. 12 and 13 to determine the functions R_p and R_i, which then are used with Eq. 1 to calculate the mean level reflectance.

Modeling the P_p Probability Function

Models based on light scattering in paper generally use an empirical expression for MTF or PSF such as shown in Eqs. 3 and 4. Similarly, a model based on probability may employ an empirical expression for P_p. For example, the data in Fig. 3 show the measured reflectance between the dots, R_p, and the reflectance of the dots, R_i, versus F. The data are reasonably well fit by Eqs. 5 and 6. Comparing Eqs. 5 and 6 with Eqs. 12 and 13 suggests the following empirical expressions for R_p and R_i.

Due to typographic error, $P_i I_0 R_g (1–F)$ *should be read as* $P_p I_0 R_g (1–F)$

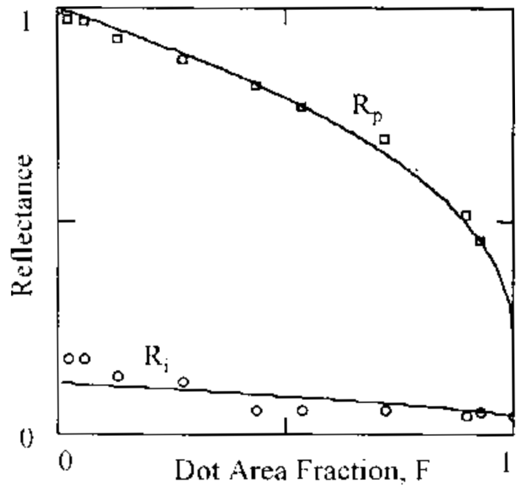

Figure 4. Empirical model with Eqs. 14, 11, 13, 12, and 1 fit to data from Fig. 3 on paper reflectance R_p and ink reflectance R_i.

$$P_p = 1 - (1 - F)^w, \quad (14)$$

$$P_i = F^w. \quad (15)$$

However, these two expressions do not relate to each other through Eq. 11 as they should. Thus, we might select Eq. 14 and construct P_i from Eq. 11. Then we can model the data as shown in Fig. 4, where w has been adjusted to provide the best fit to R_p versus F. Unfortunately, R_i versus F does not fit well. As an alternative, we can select Eq. 15 and solve Eq. 11 for P_p. Then we can model the data as shown in Fig. 5, where w has been adjusted to provide the best fit to R_i versus F. Unfortunately, R_p versus F does not fit well. Thus, the empirical model suggested previously does not quite agree with the requirements of the probability model.

Equation 14 seems to model the data well as F approaches 1, and Eq. 15 seems to model the data as F approaches 0. A combination of Eqs. 14 and 15 can be constructed that is in agreement with the probability model. This is done by first defining the following functions:

$$PP1 = 1 - (1 - F)^w, \quad (16)$$

$$PI1 = 1 - PP1\left(\frac{1-F}{F}\right), \quad (17)$$

$$PI2 = F^w, \quad (18)$$

$$PP2 = (1 - PI2)\left(\frac{F}{1-F}\right). \quad (19)$$

We then combine them so Eq. 14 dominates at high F and Eq. 15 dominates at low F.

$$P_p = F \cdot PP1 + (1 - F)\, PP2, \quad (20)$$

$$P_i = F \cdot PI1 + (1 - F)PI2. \quad (21)$$

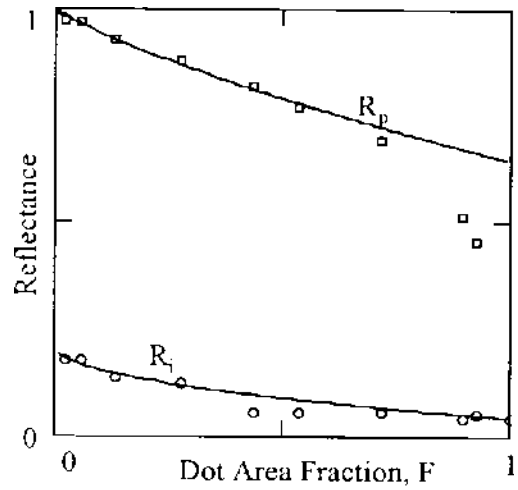

Figure 5. Empirical model with Eqs. 15, 11, 13, 12, and 1 fit to data from Fig. 3 on paper reflectance, R_p and ink reflectance R_i.

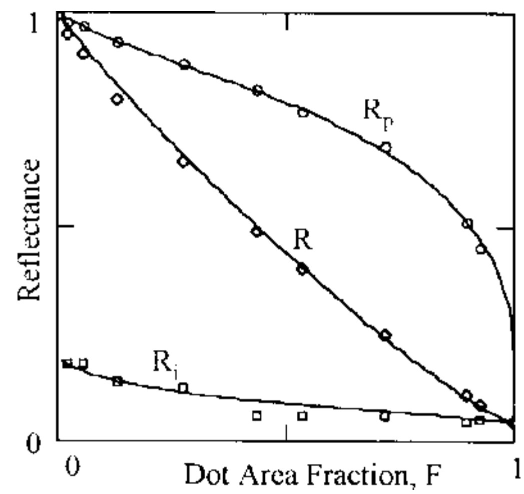

Figure 6. Empirical model with Eqs. 22, 11, 13, 12, and 1 fit to data from Fig. 3 on paper reflectance R_p and ink reflectance R_i.

With some algebra it can be shown that these two expressions for P_p and P_i do relate as they should through Eq. 11 and thus are consistent with the probability model of halftone imaging. Equation 20 can be developed into the following equivalent expression:

$$P_p = F[1 - (1 - F)^w + (1 - F^w)]. \quad (22)$$

Then Eq. 22, combined with Eqs. 11, then 5 and 6, and then 1 results in the fit shown in Fig. 6. This model fits the data as well as empirical Eqs. 5 and 6 and is also consistent with the probability model.

Conclusion

Probability-based models of the Yule-Nielsen effect offer some advantages over models based on the paper MTF or PSF functions. They are more intuitively described and understood, and they are generally expressed as simple, algebraic functions. The disadvantage of probability-based modeling is that the form of the probability function P_p will be different for various halftone patterns. However, this may not be a significant drawback compared to traditional models based on PSF because a geometric function for the specific halftone pattern must be known to apply a PSF model. In addition, deriving the P_p function from a convolution between the geometric halftone pattern and the paper PSF should be possible.[18] An alternative possibility is the development of experimental relationships, such as Eq. 7, to relate the probability models for a particular digital halftone pattern of interest to the spread function of light in paper. Further work is underway in this laboratory to explore these relationships experimentally.

References

1. A. Murray, *J. Franklin Inst*. **221**, 721 (1936).
2. J. A. Yule and W. J. Nielsen, *TAGA Proc*. 65 (1951).
3. F. R. Clapper and J. A. Yule, *J. Opt. Soc. Am*. **43**, 600 (1953).
4. J. A. Yule, D. J. Howe, and J. H. Altman, *TAPPI* **50,** 337 (1967).
5. F. Ruckdeschel and O. G. Hauser, *Appl. Opt.* **17**, 3376 (1978).
6. J. R . Huntsman, *J. Imag. Tech*. **13**, 136 (1987).
7. J. S. Arney, P. G. Engeldrum, and H. Zeng, *J. Imag. Sci. Technol*. **39,** 502 (1995); ***see pg. 35, this publication***.
8. J. S. Arney, C. D. Arney, and P. G. Engeldrum, *J. Imag. Sci. Technol*. **40,** 233 (1996); ***see pg. 432, this publication***.
9. M. Wedin and B. Kruse, *Proc.SPIE* **2413**, (1995).
10. B. Kruse and M. Wedin, *TAGA Proc*. 329 (1995).
11. S. Gustavson, in *Proc. of IS&T Conference on Digital Printing*, Springfield, VA 1996, p. 111.
12. M. Maltz, *J. Appl. Photogr. Eng*. **9,** 83 (1983).
13. P. Oittinen, *Adv. in Printing Sci. & Tech*. W. H. Banks, Ed, **16**, 121 (1982).
14. P. G. Engeldrum and B. Pridham, *TAGA Proc*. (1995).
15. J. S. Arney, C. D. Arney, and M. Katsube, *J. Imag. Sci. Technol*. **40,** 19 (1996).
16. J. C. Dainty and R. Shaw, *Image Science*, Academic Press, London (1974) p. 258.
17. Peter G. Engeldrum, *J. Imag. Sci. Technol*. **38**, 545 (1994); ***see pg. 383, this publication***.
18. G. Rogers, Optical Dot Gain in Halftone Print, *J. Imag. Sci. Tech.* **41,** 643 (1997); ***see pg. 462, this publication;*** and Optical Dot Gain: Lateral Scattering Probabilities, , *J. Imag. Sci. Tech.* **42**(4) 341 (1998); ***see pg. 495, this publication.***

❋ Previously published in the *Journal of Imaging Science and Technology* **41**(6), pp. 633–636, 1997.